

# ITERATIVE BILINEAR TEMPORAL-SPECTRAL FUSION FOR UNSUPERVISED REPRESENTATION LEARNING IN TIME SERIES

**Anonymous authors**

Paper under double-blind review

## ABSTRACT

Unsupervised representation learning for multivariate time series has practical significances, but it is also a challenging problem because of its complex dynamics and sparse annotations. Existing works mainly adopt the framework of contrastive learning and involve the data augmentation techniques to sample positives and negatives for contrastive training. However, their designs of representation learning framework have two drawbacks. First, we revisit the augmentation methods for time series of existing works and note that they mostly use segment-level augmentation derived from time slicing, which may bring about sampling bias and incorrect optimization with false negatives due to the loss of global context. Second, they all pay no attention to incorporate the spectral information and temporal-spectral relations in feature representation. To address these problems, we propose a novel framework, namely Bilinear Temporal-Spectral Fusion (BTSF). In contrast to segment-level augmentation, we utilize the instance-level augmentation by simply applying dropout on the entire time series for better preserving global context and capturing long-term dependencies. Also, an iterative bilinear temporal-spectral fusion module is devised to explicitly encode the affinities of abundant time-frequency pairs and iteratively refine representations of time series through cross-domain interactions with Spectrum-to-Time (S2T) and Time-to-Spectrum (T2S) Aggregation modules. Finally, we make sufficient assessments including alignment and uniformity to prove the effectiveness of our bilinear feature representations produced by BTSF. Extensive experiments are conducted on three major practical tasks for time series such as classification, forecasting and anomaly detection, which is the first to evaluate on all three tasks. Results shows that our BTSF achieves the superiority over the state-of-the-art methods and surpasses them by a large margin across downstream tasks. Code will be released.

## 1 INTRODUCTION

Time series analysis (Oreshkin et al., 2020) plays a crucial role in various real-world scenarios, such as traffic prediction, clinical trials and financial market. Classification Esling & Agon (2012), forecasting (Deb et al., 2017) and anomaly detection (Laptev et al., 2015) are main tasks for time series analysis. However, there is often no adequate labeled data for training and results are not ideal when time series are sparsely labeled or without supervision (Hyvarinen & Morioka, 2016a; Lan et al., 2021). Therefore, it is valuable to study on the unsupervised representation learning for time series with which the learned representations can be used for aforementioned downstream tasks. Unsupervised representation learning has been well studied in computer vision and natural language processing (Denton & Birodkar, 2017; Gutmann & Hyvärinen, 2012; Wang & Gupta, 2015; Pagliarini et al., 2018; Chen et al., 2020b) but only a few researches are related with time series analysis (Eldele et al., 2021b; Yue et al., 2021; Liu et al., 2021). Recent works mainly utilize the contrastive learning framework (Chen et al., 2020a; Zerveas et al., 2021) for unsupervised representation learning in time series. Inspired by Word2Vec (Mikolov et al., 2013), Scalable Representation Learning (SRL) (Franceschi et al., 2019) proposes a novel triplet loss and tries to learn scalable representations via randomly sampling time segments. Contrastive Predictive Coding (CPC) (Oord et al., 2018) conducts representation learning by using powerful autoregressive models in latent space to

make predictions in the future, relying on Noise-Contrastive Estimation (Gutmann & Hyvärinen, 2010) for the loss function in similar ways. Temporal and Contextual Contrasting (TS-TCC) (Eldede et al., 2021b) is an improved work of CPC and learns robust representation by a harder prediction task against perturbations introduced by different timestamps and augmentations. Temporal Neighborhood Coding (TNC) (Tonekaboni et al., 2021) presents a novel neighborhood-based unsupervised learning framework and applies sample weight adjustment for non-stationary multivariate time series. Their main difference is that they select contrastive pairs according to different sampling policies based on time slicing. However, such policy is prone to be affected by false negatives and fails to capture long-term dependencies because of the loss of a global semantical information. Besides they only extract temporal feature and neglect to leverage spectral feature and involve temporal-spectral relations, which may affect the performance.

We implement existing works according to public codes. Figure 1 shows statistics about false predictions on time series classification. Specifically, "by spectral" means we use the sampling methods proposed by previous works to generate contrastive pairs but transform the sampled time series into spectral domain to extract feature for later contrastive training and testing. It is notable that existing works all have a low overlap percentage around 30% about false predictions with only temporal or spectral feature. The phenomenon demonstrates their temporal

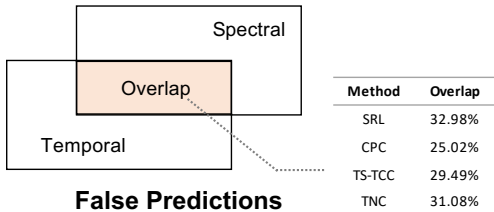


Figure 1: Statistics about false predictions of 5000 randomly selected evaluation samples.

and spectral representations are learned independently. Therefore, if temporal and spectral features could be simultaneously utilized and achieve alignment, performance of learned representations would be better. Based on the aforementioned shortcomings of existing works, we propose an unsupervised representation learning framework for multivariate time series, namely Bilinear Temporal-Spectral Fusion (BTSF). BTSF promotes the representation learning process from two aspects, the more reasonable construction of contrastive pairs and the full integration of temporal and spectral information. In order to preserve the global temporal information and have the ability to capture long-term dependencies of time series, BTSF uses the entire time series as input and simply applies a standard dropout (Srivastava et al., 2014) as an instance-level augmentation to produce different views of time series. Such construction of contrastive pairs ensures that the augmented time series would not change their raw properties, which effectively reduces the possible false negatives and positives. Considering the effective combination of temporal and spectral information in feature representation, we perform an iterative bilinear fusion between temporal and spectral features to produce a fine-grained second-order feature which explicitly preserves abundant pairwise temporal-spectral affinities. To utilize the informative affinities, we further design a cross-domain interaction with Spectrum-to-Time and Time-to-Spectrum Aggregation modules to iteratively refine temporal and spectral features for cycle update. Compared to simple combination operations like summation and concatenation, our bilinear fusion makes it possible that the temporal (spectral) feature gets straightly enhanced by spectral (temporal) information of the same time series, which is proved to be effective by our further experiments and analysis.

Our main contributions are summarized as the following:

- We revisit the construction of contrastive pairs in existing works for unsupervised representation learning in time series and propose the standard dropout as a simple but effective instance-level augmentation to augment the entire time series, maximumly preserving global contextual information and outperforming existing time slicing based methods (segment-level augmentation).
- A novel representation learning framework BTSF is proposed to explicitly model pairwise temporal-spectral dependencies with iterative bilinear fusion which not only simultaneously leverages global contextual information in two domains but also iteratively refines cross-domain feature representation for time series in a new fusion-and-squeeze manner.
- Sufficient assessments are conducted to identify the generalization ability of our learned representations. Besides classification, we also evaluate the model on other downstream tasks like forecasting and anomaly detection, which is the first to experiments on all three tasks. Results

show that our BTSF not only largely outperforms existing works but also is competitive with supervised techniques.

## 2 RELATED WORK

**Unsupervised representation learning for time series** A relevant direction of research about representation learning on sequence data has been well-studied (Chung et al., 2015; Fraccaro et al., 2016; Krishnan et al., 2017; Bayer et al., 2021). However, few efforts have made in unsupervised representation learning for time series (Långkvist et al., 2014; Eldele et al., 2021b; Yue et al., 2021). Applying auto-encoders (Choi et al., 2016) and seq-to-seq models (Malhotra et al., 2017; Lyu et al., 2018) with an encoder-decoder architecture to reconstruct the input are preliminary approaches to unsupervised representation learning for time series. Rocket (Dempster et al., 2020) is a fast method that involves training a linear classifier on top of features extracted by a flat collection of numerous and various random convolutional kernels. Several approaches leverage inherent correlations in time series to learn unsupervised representations. SPIRAL (Lei et al., 2017) bridges the gap between time series data and static clustering algorithm through preserving the pairwise similarities of the raw time series data. Ma et al. (2019) integrates the temporal reconstruction and K-means (Krishna & Murty, 1999) objective to generate cluster-specific temporal representations. Another group of approaches design different sample policy and incorporate contrastive learning (Chen et al., 2020a; Hyvarinen & Morioka, 2016b;a; Oord et al., 2018) to tackle representation learning for temporal data without supervision. Time-Contrastive Learning (TCL) (Hyvarinen & Morioka, 2016a), Contrastive Predictive Coding (CPC) (Oord et al., 2018), Scalable Representation Learning (SRL) (Franceschi et al., 2019), Temporal and Contextual Contrasting (TS-TCC) (Eldele et al., 2021b) and Temporal Neighborhood Coding (TNC) (Tonekaboni et al., 2021) are all segment-level methods which sample contrastive pairs along temporal axis. TST (Zerveas et al., 2021) apply a transformer-based model (Vaswani et al., 2017) to unsupervised representation learning of multivariate time series. Nevertheless, they all fail to utilize the temporal-spectral affinities in time series.

**Second-order pooling** Second-Order Pooling (Carreira et al., 2012) is first proposed to preserve spatial information about pairwise correlations in semantic segmentation (Long et al., 2015). Similar approach called Bilinear CNNs (Lin et al., 2015) first leverages a pooled outer product of features to solve fine-grained visual recognition tasks (Akata et al., 2015). Due to the good property of bilinear feature (Gao et al., 2020), many approaches (Wei et al., 2018; Yu et al., 2018) have been devised for fine-grained image classification tasks to exploit rich spatial relations. CBP (Gao et al., 2016) enhances the applicability to computationally complex tasks with reducing the feature dimensionality. MCBP (Fukui et al., 2016) applies compact bilinear pooling to Visual Question Answering (Antol et al., 2015). FBM (Li et al., 2017) considers the pairwise feature relations with linear complexity and Hadamard Product (Kim et al., 2016) further approximates full bilinear pooling to and takes advantage of the expanded representations with low-rank bilinear pooling (Amin et al., 2020). However, these second-order pooling methods fail to adaptively refine the final feature due to the one-shot fusion process. And no research has been done to exploit the use of bilinear pooling for time series analysis.

## 3 METHOD

### 3.1 RETHINKING THE CONSTRUCTION OF CONTRASTIVE PAIRS

Previous researches on the unsupervised representation learning for time series mainly tackle the problem by designing different sampling policy on temporal data. They use the sampled data to construct the contrastive objective for guiding the training procedure. Sampling bias is an inevitable problem for existing representation works in time series because of their segment-level sampling policy (time slicing). Time slicing is unable to capture the long-term dependencies due to the loss of global semantical information. To explore an effective augmentation method for the construction of contrastive pairs, we first investigate general augmentation methods for time series. A latest empirical survey (Iwana & Uchida, 2021a) evaluates 12 time series data augmentation methods on 128 time series classification datasets with 6 different types of neural networks. According to results, no augmentation method, not excepting time slicing, is able to improve performance on all datasets consistently. It is because time series is sensitive to sequential order and temporal patterns.

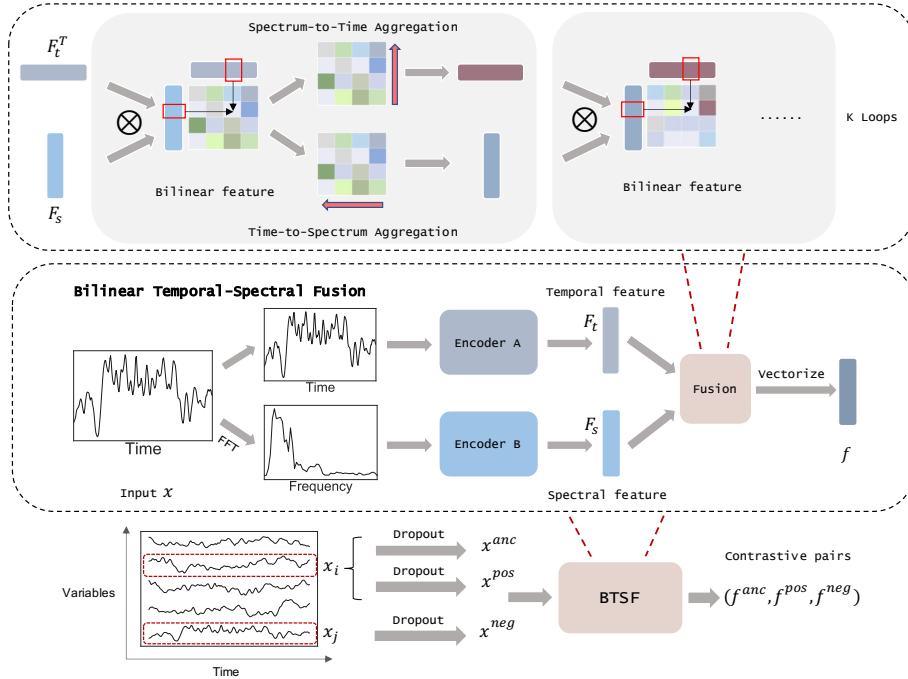


Figure 2: The diagram of our general unsupervised representation learning framework for multivariate time series,  $\otimes$  is the cross product. See Section 3.2 for more details.

To preserve the global temporal information and not change the original properties for time series, we apply a standard dropout as a minimal data augmentation to generate different views in unsupervised representation learning. Specifically, we simply employ two independently sampled dropout masks on the time series to obtain a positive pair and treat time series of other variables as negative samples for negative pairs construction. With the instance-level contrastive pairs, our method has the ability to capture long-term dependencies and effectively reduce the sampling bias which is superior to previous segment-level pairs.

In the procedure of contrastive pairs construction, we pass the each time series  $\mathbf{x}$  to the dropout to generate a positive pair  $\mathbf{x}^{anc}$  and  $\mathbf{x}^{pos}$ .

$$\mathbf{x}^{anc} = Dropout(\mathbf{x}), \quad \mathbf{x}^{pos} = Dropout(\mathbf{x}), \tag{1}$$

For negative samples, we randomly choose other variables as  $\mathbf{x}^{neg}$  for multivariate time series. Due to the nature of our augmentation method, our framework is general and becomes independent of the states of time series which means that we can process both non-stationary and periodic time series. In contrast, time slicing fails to deal with the periodic time series because it is possible for them to choose false negative samples. The dropout rate is set to 0.1 in our experiments. For experiment comparisons with other augmentation methods and the choices of dropout rate, see Appendix A.3

### 3.2 ITERATIVE BILINEAR TEMPORAL-SPECTRAL FUSION

In this subsection, we provide a detailed introduction to a general and effective framework for learns a discriminative feature representation for multivariate time series, namely Bilinear Temporal-Spectral Fusion (BTSF). As illustrated in Figure 2, after constructing the contrastive pairs, we map the time series to a high dimensional feature space to assimilate  $\mathbf{x}$  and  $\mathbf{x}^{pos}$ , and to distinguish  $\mathbf{x}^{neg}$  from  $\mathbf{x}$ . Previous works neglect to leverage spectral feature and temporal-spectral relations, our proposed BTSF not only simultaneously utilize spectral and temporal features but also enhances the representation learning in a more fine-grained way. Instead of summation and concatenation, BTSF adopts iterative bilinear temporal-spectral fusion to iteratively explore and refine the pairwise affinities between temporal and spectral features for producing an interactive feature representation, representing the most common parts of positive pairs and enlarging the differences of negative pairs.

Specifically, each augmented time series  $\mathbf{x}_t$  is first transformed to spectral domain by a fast Fourier transform (FFT), obtaining spectral signal  $\mathbf{x}_s$ . Then  $\mathbf{x}_t$  and  $\mathbf{x}_s$  are delivered to two encoding networks for feature extraction respectively. The process is as the following:

$$\mathbf{F}_t = \text{Encoder}_A(\mathbf{x}_t; \boldsymbol{\theta}_t), \quad \mathbf{F}_s = \text{Encoder}_B(\mathbf{x}_s; \boldsymbol{\theta}_s) \quad (2)$$

where  $\mathbf{F}_t \in \mathbb{R}^{m \times d}$  and  $\mathbf{F}_s \in \mathbb{R}^{n \times d}$  are temporal and spectral features,  $\boldsymbol{\theta}_t$  and  $\boldsymbol{\theta}_s$  are parameters of their encoding networks  $\text{Encoder}_A$  and  $\text{Encoder}_B$  respectively. We just use simple stacks of dilated causal convolutions (Bai et al., 2018) to encode temporal features and use 1D convolutional blocks to extract spectral features. We apply a max-pooling layer in the end of encoding network to guarantee the same size of features, which makes our model scalable to input length. BTSF makes an iterative bilinear fusion between  $\mathbf{F}_t$  and  $\mathbf{F}_s$ . Specifically, we establish a channel-wise interaction between features of two domains as the following:

$$\mathbf{F}(i, j) = \mathbf{F}_t(i)^T \mathbf{F}_s(j) \quad (3)$$

where  $i$  and  $j$  stand for the  $i$ -th and  $j$ -th location in temporal and spectral axes respectively. This bilinear process adequately models the fine-grained time-frequency affinities between  $\mathbf{F}_t(i) \in \mathbb{R}^d$  and  $\mathbf{F}_s(j) \in \mathbb{R}^d$ . To summarize such affinities globally, BTSF integrates the obtained feature  $\mathbf{F}(i, j) \in \mathbb{R}^{d \times d}$  to produce the initial bilinear feature vector  $\mathbf{F}_{bilinear} \in \mathbb{R}^{d \times d}$  with sum pooling of all time-frequency feature pairs:

$$\mathbf{F}_{bilinear} = \mathbf{F}_t^T \mathbf{F}_s = \sum_{i=1}^m \sum_{j=1}^n \mathbf{F}(i, j) = \sum_{i=1}^m \sum_{j=1}^n \mathbf{F}_t(i)^T \mathbf{F}_s(j) \quad (4)$$

where  $\mathbf{F}_t^T \mathbf{F}_s$  uses the outer product. This bilinear feature conveys the fine-grained time-frequency affinities to acquire a more discriminative feature representation. Then we encode cross-domain affinities to adaptively refine the temporal and spectral features through an iterative procedure.

$$\begin{aligned} \text{S2T} : \quad \mathbf{F}_t &= \text{BiCasual}(\text{Conv}(\mathbf{F}_{bilinear})) \\ \text{T2S} : \quad \mathbf{F}_s &= \text{Conv}(\text{BiCasual}(\mathbf{F}_{bilinear})) \end{aligned} \quad (5)$$

where  $\mathbf{F}_t \in \mathbb{R}^{m \times d}$  and  $\mathbf{F}_s \in \mathbb{R}^{n \times d}$  are updated by Spectrum-to-Time Aggregation (S2T :  $\mathbb{R}^{d \times d} \rightarrow \mathbb{R}^{m \times d}$ ) and Time-to-Spectrum Aggregation (T2S :  $\mathbb{R}^{d \times d} \rightarrow \mathbb{R}^{n \times d}$ ).  $\text{Conv}$  is normal convolutional blocks and  $\text{BiCasual}$  is bi-directional casual convolutional blocks. Specifically, S2T first aggregates spectrum-attentive information for each temporal feature through applying convolutional blocks along spectral axis. Then it exchanges the spectrum-related information along temporal axis to refine the temporal features by several bi-directional casual convolutions. Contrary to S2T, T2S applies above aggregation-exchange procedure from temporal domain to spectral domain. S2T and T2S modules adequately aggregate the cross-domain dependencies and refine the temporal and spectral features respectively. In turn, refined temporal and spectral features are able to produce more discriminative bilinear feature. S2T, T2S and bilinear fusion jointly form a loop block. After several loops of Eq.(4) and Eq.(5), the final bilinear feature  $\mathbf{F}_{bilinear}$  is obtained. The ablation study of loops number is in Appendix A.3.

Nevertheless, its efficiency may suffer from the memory overhead of storing high-dimensional features with the quadratic expansion. To solve the problem, we transform the final bilinear feature into a low-rank one by inserting and factorizing an interaction matrix  $\mathbf{W} \in \mathbb{R}^{m \times n}$ . It is first inserted to make linear transformation between each temporal-spectral feature pair:

$$\mathbf{F}_{bilinear} = \mathbf{F}_t^T \mathbf{W} \mathbf{F}_s = \sum_{i=1}^m \sum_{j=1}^n \mathbf{F}_t(i)^T \mathbf{W}(i, j) \mathbf{F}_s(j) \quad (6)$$

where  $\circ$  denotes Hadamard product. Then, we use  $\mathbf{W} = \mathbf{U}\mathbf{V}^T$  to factorize the interaction matrix into  $\mathbf{U} \in \mathbb{R}^{m \times l}$  and  $\mathbf{V}^{n \times l}$  with  $l \ll d$ . The low-rank bilinear feature can be reformulated:

$$\mathbf{F}_{bilinear} = \mathbf{F}_t^T \mathbf{U}\mathbf{V}^T \mathbf{F}_s = \mathbf{U}^T \mathbf{F}_t \circ \mathbf{V}^T \mathbf{F}_s \quad (7)$$

where BTSF employs the two linear mappings without biases to produce the bilinear representations  $\mathbf{F}_{bilinear} \in \mathbb{R}^{l \times d}$  for a given output dimension  $l$ . Through this process, the storing memory of naïve features of Eq.(4) is reduced largely from  $O(d^2)$  to  $O(ld)$ .

Table 1: Comparisons of classification results on all UCR and UEA datasets.

Methods	UCR datasets		UEA datasets	
	Average Accuracy	Average Rank	Average Accuracy	Average Rank
Supervised	89.67	1.67	82.04	1.54
KNN	73.81	4.68	67.81	2.77
SRL	81.24	3.27	68.30	2.37
CPC	80.57	3.54	65.84	2.59
TS-TCC	82.75	2.68	69.43	2.11
TNC	79.95	2.27	70.58	2.25
<b>BTSF</b>	<b>92.11</b>	<b>1.33</b>	<b>86.72</b>	<b>1.26</b>

For not forgetting the original temporal and spectral information, the initial temporal feature  $\mathbf{F}_t \in \mathbb{R}^{l \times d}$  and spectral feature  $\mathbf{F}_s \in \mathbb{R}^{l \times d}$  are both combined with  $\mathbf{F}_{bilinear}$  to enhance the representative capacity. Therefore, the final joint feature representation  $\mathbf{f} \in \mathbb{R}^{l \times d}$  of each augmented time series can be expressed as the following:

$$\begin{aligned}
 \mathbf{f} &= \sigma(\mathbf{F}_t + \mathbf{F}_s + \mathbf{F}_{bilinear}) \\
 &= \sigma(\mathbf{W}_t^T \mathbf{F}_t + \mathbf{W}_s^T \mathbf{F}_s + \mathbf{F}_t^T \mathbf{W} \mathbf{F}_s) \\
 &= \sigma(\mathbf{W}_t^T \mathbf{F}_t + \mathbf{W}_s^T \mathbf{F}_s + \mathbf{U}^T \mathbf{F}_t \circ \mathbf{V}^T \mathbf{F}_s)
 \end{aligned} \tag{8}$$

where  $\mathbf{W}_t \in \mathbb{R}^{m \times l}$  and  $\mathbf{V}_t \in \mathbb{R}^{m \times l}$  are all linear transformation layers.  $\sigma$  is the sigmoid function. After vectorizing the feature representations  $\mathbf{f}^{anc}$ ,  $\mathbf{f}^{pos}$  and  $\mathbf{f}^{neg}$  of a contrastive tuple  $(\mathbf{x}^{anc}, \mathbf{x}^{pos}, \mathbf{x}^{neg})$ , we build a loss function to minimize and maximize the distance of positive and negative pairs respectively. We represent a multivariate time series as  $\mathbf{X} \in \mathbb{R}^{D \times T} = \{\mathbf{x}_j\}_{j=1}^D$ , where  $D$  is the number of variables and  $T$  is the length of time series. Thus, the contrastive loss for a training batch of multivariate time series can be expressed as the following:

$$\mathcal{L} = \mathbb{E}_{\mathbf{X} \sim \mathcal{P}_{data}} [-\log(\text{sim}(\mathbf{f}^{anc}, \mathbf{f}^{pos})/\tau) + \mathbb{E}_{\mathbf{x}^{neg} \sim \mathbf{X}} [\log(\text{sim}(\mathbf{f}^{anc}, \mathbf{f}^{neg})/\tau)]] \tag{9}$$

where  $\text{sim}(\cdot, \cdot)$  denotes the inner product to measure the distance between two  $\ell_2$  normalized feature vectors and  $\tau$  is a temperature parameter. Eq.(9) demonstrates that for each multivariate time series, when a time series is chosen for constructing the positive pair, time series of all other variables are the negative samples. For ablation studies of hyperparameters, see Appendix A.3.

## 4 EXPERIMENTS

We apply our BTSF on multiple time series datasets in three major practical tasks including classification, anomaly detection and forecasting. It is noted that we are the first to evaluate on all three tasks. We compare our performances with state-of-the-art approaches for unsupervised representation learning for time series: Contrastive Predictive Coding (CPC) (Oord et al., 2018), Scalable Representation Learning (SRL) (Franceschi et al., 2019), Temporal and Contextual Contrasting (TS-TCC) (Eldede et al., 2021b) and Temporal Neighborhood Coding (TNC) (Tonekaboni et al., 2021). For fair comparisons, we implement these methods by public code with the same encoder architecture and the similar computational complexity and parameters, also use the same representation dimensions with BTSF. More specific descriptions of tasks definitions, datasets and experiments can be found in Appendix A.4.

**Classification** We evaluate our learned representation on downstream classification tasks for time series with widely-used time series classification datasets (Anguita et al., 2013; Goldberger et al., 2000; Andrzejak et al., 2001; Moody, 1983; Dau et al., 2019; Bagnall et al., 2018). For fair comparisons, we further train a linear classifier on top of the learned representations to evaluate how well the representations can be used to classify hidden states, following Tonekaboni et al. (2021). Beyond aforementioned methods, we also implement a K-nearest neighbor classifier equipped with DTW (Chen et al., 2013) metric and a supervised model which is trained with the same encoder and classifier with those of our unsupervised model. In the training stage, we keep the original train/test



Table 2: Comparisons of classification results.

Methods	HAR		Sleep-EDF		ECG Waveform	
	Accuracy	AUPRC	Accuracy	AUPRC	Accuracy	AUPRC
Supervised	92.03±2.48	0.98±0.00	83.41±1.44	0.78±0.52	94.81±0.28	0.67±0.01
KNN	84.85±0.84	0.75±0.01	64.87±1.73	0.75±2.88	54.76±5.46	0.38±0.06
SRL	63.60±3.37	0.71±0.01	78.32±1.45	0.71±2.83	75.51±1.26	0.47±0.00
CPC	86.43±1.41	0.93±0.01	82.82±1.68	0.73±2.15	68.64±0.49	0.42±0.01
TS-TCC	88.04±2.46	0.92±0.02	83.00±0.71	0.74±2.63	74.81±1.10	0.53±0.02
TNC	88.32±0.12	0.94±0.01	82.97±0.94	0.76±1.73	77.79±0.84	0.55±0.01
<b>BTSF</b>	<b>94.63±0.14</b>	<b>0.99±0.01</b>	<b>87.45±0.54</b>	<b>0.82±0.48</b>	<b>98.12±0.14</b>	<b>0.72±0.01</b>

Table 3: Comparisons of multivariate forecasting results.

Datasets	Length	Supervised		SRL		CPC		TS-TCC		TNC		BTSF	
		MSE	MAE	MSE	MAE	MSE	MAE	MSE	MAE	MSE	MAE	MSE	MAE
ETTh1	48	0.685	0.625	0.758	0.711	0.779	0.768	0.720	0.693	0.705	0.688	<b>0.613</b>	<b>0.524</b>
	168	0.931	0.752	1.341	1.178	1.282	1.083	1.129	1.044	1.097	0.993	<b>0.640</b>	<b>0.532</b>
	720	1.215	0.896	1.892	1.566	1.803	1.761	1.603	1.206	1.604	1.118	<b>0.993</b>	<b>0.712</b>
ETTh2	48	1.451	1.001	1.854	1.542	1.732	1.440	1.701	1.378	1.689	1.311	<b>0.544</b>	<b>0.527</b>
	168	3.389	1.515	5.062	2.167	4.591	3.126	3.956	2.301	3.792	2.029	<b>1.669</b>	<b>0.875</b>
	720	3.467	1.473	5.301	3.207	5.191	2.781	4.732	2.345	4.501	2.410	<b>2.566</b>	<b>1.276</b>
ETTh1	48	0.494	0.503	0.701	0.697	0.727	0.706	0.671	0.665	0.623	0.602	<b>0.395</b>	<b>0.387</b>
	96	0.678	0.614	0.901	0.836	0.851	0.793	0.803	0.724	0.749	0.731	<b>0.438</b>	<b>0.399</b>
	672	1.192	0.926	2.042	1.803	1.962	1.797	1.838	1.601	1.822	1.692	<b>0.721</b>	<b>0.643</b>
Weather	48	0.395	0.459	0.751	0.883	0.720	0.761	0.647	0.691	0.608	0.626	<b>0.366</b>	<b>0.427</b>
	168	0.608	0.567	1.204	1.032	1.351	1.067	1.117	0.962	1.081	0.970	<b>0.543</b>	<b>0.477</b>
	720	0.831	0.731	2.281	1.994	2.109	1.861	1.850	1.566	1.401	1.193	<b>0.601</b>	<b>0.522</b>

splits of datasets and use the training set to train all the models. We apply two metrics for evaluation, the prediction accuracy and the area under the precision-recall curve (AUPRC). Table 9 and Table 2 demonstrates our superior performance over existing methods in all datasets and our BTSF surpasses the supervised method, which shows that BTSF adequately leverages the temporal and spectral information in time series for representation learning. In addition, the pair-wise temporal-spectral fusion provides more fine-grained information (see Appendix A.1 for visualization results).

**Forecasting** We evaluate our algorithm with other methods on time series forecasting task in both short-term and long-term settings, following Zhou et al. (2021). A decoder is added on top of learned representations to make predictive outputs. Specifically, we train a linear regression model with L2 norm penalty and use informer (Zhou et al., 2021) as our supervised comparison method. We use two metrics to evaluate the forecasting performance, Mean Square Error (MSE) and Mean Absolute Error (MAE). Table 3 demonstrates that our BTSF has the least forecasting error of different prediction lengths (short/long) across the datasets. In addition, BTSF outperforms existing methods including supervised one in a large margin especially for long time series prediction. It is noted that BTSF gets a better performance when the length of datasets increases due to the better use of global context, which makes BTSF fully capture the long-term dependencies in long time series. More comparisons and visualization results of time series forecasting are illustrated in Appendix A.4.

**Anomaly detection** To the best of our knowledge, we are the first to evaluate on anomaly detection (Su et al., 2019; Hundman et al., 2018; Goh et al., 2016; Mathur & Tippenhauer, 2016; Braei & Wagner, 2020). The results of this task assessment reflect how well the model capture the temporal trends and how sensitive to the outlier the model is for time series. We add a decoder on top of representations learned by models and reconstruct the input time series and follow the evaluation

Table 4: Comparisons of multivariate anomaly detection.

Datasets	Metric	Supervised	SRL	CPC	TS-TCC	TNC	<b>BTSF</b>
SAaT	F1	0.901	0.710	0.738	0.775	0.799	<b>0.944</b>
WADI	F1	0.649	0.340	0.382	0.427	0.440	<b>0.685</b>
SMD	F1	0.958	0.768	0.732	0.794	0.817	<b>0.972</b>
SMAP	F1	0.842	0.598	0.620	0.679	0.693	<b>0.906</b>
MSL	F1	0.945	0.788	0.813	0.795	0.833	<b>0.984</b>

settings of [Audibert et al. \(2020\)](#). For each input data point  $x_t$  and reconstructed one  $\hat{x}_t$ , if  $|\hat{x}_t - x_t| > \tau$  ( $\tau$  is a predefined threshold),  $x_t$  is an outlier. Precision (P), Recall (R), and F1 score (F1) were used to evaluate anomaly detection performance and we just list the results of F1 metric here (see Appendix A.4 for more results of P and R metrics). Table 4 illustrates that BTSF achieves new SOTA across all datasets and especially surpasses the supervised results by a large margin. It conveys that BTSF is more sensitive to the outliers in time series since it captures long-term dynamics and expresses the fine-grained information through iterative bilinear fusion.

## 5 ANALYSIS

**Augmentation comparisons** To further prove the effectiveness of our instance-level augmentation (dropout), we compare our method with 12 other augmentation policies as mentioned in [Iwana & Uchida \(2021a\)](#): Jittering, Rotation, Scaling, Magnitude Warping, Permutation, Slicing, Time Warping, Window Warping, SPAWNER ([Kamycki et al., 2020](#)), Weighted DTW Barycentric Averaging (wDBA) ([Forestier et al., 2017](#)), Random Guided Warping (RGW) ([Iwana & Uchida, 2021b](#)) and Discriminative Guided Warping (DGW) ([Iwana & Uchida, 2021b](#)). The classification accuracy comparisons of different augmentations on HAR datasets are illustrated in Figure 3. It is noted that proposed instance-level augmentation (dropout) has a best performance in both average accuracy and variance, which demonstrates dropout is a more accurate and more stable augmentation policy for unsupervised representation learning in time series.

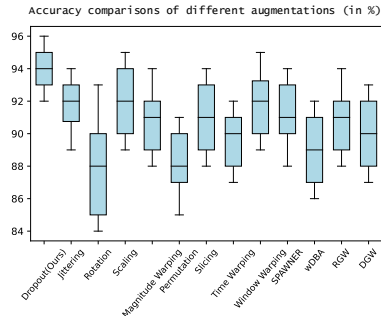


Figure 3: Classification accuracies and variances of different augmentations on HAR dataset.

**Impact of iterative bilinear fusion** To investigate the impact of iterative bilinear fusion in BTSF, we follow the experiment as illustrated in Section 1. We apply the learned representations of models to the classification task and make statistics about false predictions by only using temporal or spectral feature respectively. Specifically, we use the feature out of S2T and T2S module as temporal and spectral feature respectively. From Table 5, we find that after adding iterative bilinear fusion, BTSF not only gets a large promotion in accuracy but also achieves a good alignment between temporal and spectral domain with a overlap percentage of **96.60%**, much higher than existing works (around **30%**). Therefore, our designed iterative bilinear fusion make an effective interaction between two domains and it is vital for final prediction accuracy. More ablation studies about BTSF are in Appendix A.3.

**Alignment and uniformity** To make a comprehensive assessment of the representations, we evaluate the two properties of learned representations, *alignment* and *uniformity* ([Wang & Isola, 2020](#)). *Alignment* is used to measure the similarities of features between similar samples, which means features of a positive pair should be invariant to the noise. *Uniformity* assumes that a well-learned



Table 5: Statistics about false predictions of all test samples on HAR dataset

	Only Temporal	Only Spectral	Overlap (% by Temporal, % by Spectral)
SRL	1073	1174	349 (32.53%, 29.73%)
CPC	401	448	106 (26.43%, 23.66%)
TS-TCC	354	383	107 (30.23%, 27.94%)
TNC	346	376	115 (33.24%, 30.59%)
<b>BTSF</b>	<b>159</b>	<b>163</b>	<b>152 (96.60%, 93.25%)</b>

feature distribution should preserve maximal information as much as possible. It makes sense that well-generalized feature representations not only minimize the intra-similarities of positive pairs and enlarge the inter-distances of negative pairs but also keep the feature distributed uniformly to retain enough information. Therefore we follow Wang & Isola (2020) to make the assessments. Figure 4 and Figure 5 show the results of alignment and uniformity respectively. Compared with previous SOTA TNC and supervised results, our BTSF gets the highest mean value about feature distance of positive pairs, which means that BTSF achieves the best alignment. Additionally, the feature extracted by BTSF is evenly distributed in the encoding space which preserves maximal information of the data, much better than TNC and supervised models.

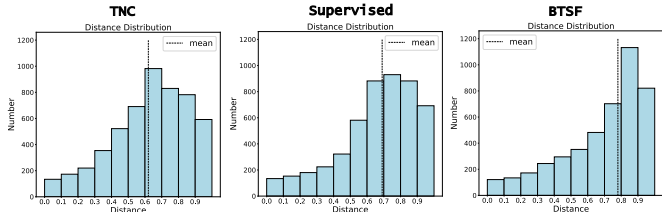


Figure 4: Distance distribution of positive pairs for assessing alignment. Our BTSF is well aligned.

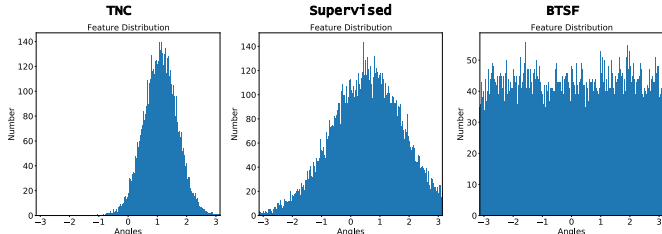


Figure 5: Feature distribution of samples in different classes on the normalized surface area for assessing uniformity. Features extracted by BTSF are evenly distributed.

## 6 CONCLUSION

In this paper, we propose Bilinear Temporal-Spectral Fusion (BTSF) for unsupervised representation learning in time series. We revisit existing representation learning methods based on contrastive framework and point out that they all fail to leverage global contextual information due to the segment-level augmentation (time slicing) and are unable to use temporal-spectral relations for enhancing representation learning. First, we utilize instance-level augmentation which use the entire time series as input and apply dropout to generate different views for training. Second, we devise iterative bilinear fusion to iteratively fuse temporal-spectral information and refine the unified feature representation for time series. The extensive experiments on classification, forecasting and anomaly detection downstream tasks have been conducted and the results demonstrates the superior performance of our BTSF. BTSF not only surpasses existing unsupervised learning models for time series in a large margin but also outperforms the supervised model across all the datasets.

## REFERENCES

- Zeynep Akata, Scott Reed, Daniel Walter, Honglak Lee, and Bernt Schiele. Evaluation of output embeddings for fine-grained image classification. In *Proceedings of the IEEE conference on computer vision and pattern recognition*, pp. 2927–2936, 2015.
- Saadullah Amin, Stalin Varanasi, Katherine Ann Dunfield, and Günter Neumann. Lower: Low-rank bilinear pooling for link prediction. In *International Conference on Machine Learning*, pp. 257–268. PMLR, 2020.
- Ralph G Andrzejak, Klaus Lehnertz, Florian Mormann, Christoph Rieke, Peter David, and Christian E Elger. Indications of nonlinear deterministic and finite-dimensional structures in time series of brain electrical activity: Dependence on recording region and brain state. *Physical Review E*, 64(6):061907, 2001.
- Davide Anguita, Alessandro Ghio, Luca Oneto, Xavier Parra, Jorge Luis Reyes-Ortiz, et al. A public domain dataset for human activity recognition using smartphones. In *Esann*, volume 3, pp. 3, 2013.
- Stanislaw Antol, Aishwarya Agrawal, Jiasen Lu, Margaret Mitchell, Dhruv Batra, C Lawrence Zitnick, and Devi Parikh. Vqa: Visual question answering. In *Proceedings of the IEEE international conference on computer vision*, pp. 2425–2433, 2015.
- Julien Audibert, Pietro Michiardi, Frédéric Guyard, Sébastien Marti, and Maria A Zuluaga. Usad: Unsupervised anomaly detection on multivariate time series. In *Proceedings of the 26th ACM SIGKDD International Conference on Knowledge Discovery & Data Mining*, pp. 3395–3404, 2020.
- Anthony Bagnall, Hoang Anh Dau, Jason Lines, Michael Flynn, James Large, Aaron Bostrom, Paul Southam, and Eamonn Keogh. The uea multivariate time series classification archive, 2018. *arXiv preprint arXiv:1811.00075*, 2018.
- Shaojie Bai, J Zico Kolter, and Vladlen Koltun. An empirical evaluation of generic convolutional and recurrent networks for sequence modeling. *arXiv preprint arXiv:1803.01271*, 2018.
- Justin Bayer, Maximilian Soelch, Atanas Mirchev, Baris Kayalibay, and Patrick van der Smagt. Mind the gap when conditioning amortised inference in sequential latent-variable models. *arXiv preprint arXiv:2101.07046*, 2021.
- Mohammad Braei and Sebastian Wagner. Anomaly detection in univariate time-series: A survey on the state-of-the-art. *arXiv preprint arXiv:2004.00433*, 2020.
- Joao Carreira, Rui Caseiro, Jorge Batista, and Cristian Sminchisescu. Semantic segmentation with second-order pooling. In *European Conference on Computer Vision*, pp. 430–443. Springer, 2012.
- Ting Chen, Simon Kornblith, Mohammad Norouzi, and Geoffrey Hinton. A simple framework for contrastive learning of visual representations. In *International conference on machine learning*, pp. 1597–1607. PMLR, 2020a.
- Ting Chen, Simon Kornblith, Mohammad Norouzi, and Geoffrey Hinton. A simple framework for contrastive learning of visual representations. In *Proceedings of the 37th International Conference on Machine Learning*, volume 119 of *Proceedings of Machine Learning Research*, pp. 1597–1607, 13–18 Jul 2020b.
- Yanping Chen, Bing Hu, Eamonn Keogh, and Gustavo EAPA Batista. Dtw-d: time series semi-supervised learning from a single example. In *Proceedings of the 19th ACM SIGKDD international conference on Knowledge discovery and data mining*, pp. 383–391, 2013.
- Edward Choi, Mohammad Taha Bahadori, Elizabeth Searles, Catherine Coffey, Michael Thompson, James Bost, Javier Tejedor-Sojo, and Jimeng Sun. Multi-layer representation learning for medical concepts. In *Proceedings of the 22nd ACM SIGKDD International Conference on Knowledge Discovery and Data Mining*, pp. 1495–1504, 2016.

- Junyoung Chung, Kyle Kastner, Laurent Dinh, Kratarth Goel, Aaron C Courville, and Yoshua Bengio. A recurrent latent variable model for sequential data. *Advances in neural information processing systems*, 28:2980–2988, 2015.
- Hoang Anh Dau, Anthony Bagnall, Kaveh Kamgar, Chin-Chia Michael Yeh, Yan Zhu, Shaghayegh Gharghabi, Chotirat Ann Ratanamahatana, and Eamonn Keogh. The ucr time series archive. *IEEE/CAA Journal of Automatica Sinica*, 6(6):1293–1305, 2019.
- Chirag Deb, Fan Zhang, Junjing Yang, Siew Eang Lee, and Kwok Wei Shah. A review on time series forecasting techniques for building energy consumption. *Renewable and Sustainable Energy Reviews*, 74:902–924, 2017.
- Angus Dempster, François Petitjean, and Geoffrey I Webb. Rocket: exceptionally fast and accurate time series classification using random convolutional kernels. *Data Mining and Knowledge Discovery*, 34(5):1454–1495, 2020.
- Emily Denton and Vighnesh Birodkar. Unsupervised learning of disentangled representations from video. *arXiv preprint arXiv:1705.10915*, 2017.
- Emadeldeen Eldele, Zhenghua Chen, Chengyu Liu, Min Wu, Chee-Keong Kwoh, Xiaoli Li, and Cuntai Guan. An attention-based deep learning approach for sleep stage classification with single-channel eeg. *IEEE Transactions on Neural Systems and Rehabilitation Engineering*, 29:809–818, 2021a.
- Emadeldeen Eldele, Mohamed Ragab, Zhenghua Chen, Min Wu, Chee Keong Kwoh, Xiaoli Li, and Cuntai Guan. Time-series representation learning via temporal and contextual contrasting. *arXiv preprint arXiv:2106.14112*, 2021b.
- Philippe Esling and Carlos Agon. Time-series data mining. *ACM Computing Surveys (CSUR)*, 45(1):1–34, 2012.
- Germain Forestier, François Petitjean, Hoang Anh Dau, Geoffrey I Webb, and Eamonn Keogh. Generating synthetic time series to augment sparse datasets. In *2017 IEEE international conference on data mining (ICDM)*, pp. 865–870. IEEE, 2017.
- Marco Fraccaro, Søren Kaae Sønderby, Ulrich Paquet, and Ole Winther. Sequential neural models with stochastic layers. *arXiv preprint arXiv:1605.07571*, 2016.
- Jean-Yves Franceschi, Aymeric Dieuleveut, and Martin Jaggi. Unsupervised scalable representation learning for multivariate time series. *Advances In Neural Information Processing Systems 32 (Nips 2019)*, 32(CONF), 2019.
- Akira Fukui, Dong Huk Park, Daylen Yang, Anna Rohrbach, Trevor Darrell, and Marcus Rohrbach. Multimodal compact bilinear pooling for visual question answering and visual grounding. *arXiv preprint arXiv:1606.01847*, 2016.
- Yang Gao, Oscar Beijbom, Ning Zhang, and Trevor Darrell. Compact bilinear pooling. In *Proceedings of the IEEE conference on computer vision and pattern recognition*, pp. 317–326, 2016.
- Zhi Gao, Yuwei Wu, Xiaoxun Zhang, Jindou Dai, Yunde Jia, and Mehrtash Harandi. Revisiting bilinear pooling: A coding perspective. In *Proceedings of the AAAI Conference on Artificial Intelligence*, volume 34, pp. 3954–3961, 2020.
- Jonathan Goh, Sridhar Adepu, Khurum Nazir Junejo, and Aditya Mathur. A dataset to support research in the design of secure water treatment systems. In *International conference on critical information infrastructures security*, pp. 88–99. Springer, 2016.
- Ary L Goldberger, Luis AN Amaral, Leon Glass, Jeffrey M Hausdorff, Plamen Ch Ivanov, Roger G Mark, Joseph E Mietus, George B Moody, Chung-Kang Peng, and H Eugene Stanley. Physiobank, physiotoolkit, and physionet: components of a new research resource for complex physiologic signals. *circulation*, 101(23):e215–e220, 2000.

- Michael Gutmann and Aapo Hyvärinen. Noise-contrastive estimation: A new estimation principle for unnormalized statistical models. In Yee Whye Teh and Mike Titterton (eds.), *Proceedings of the Thirteenth International Conference on Artificial Intelligence and Statistics*, volume 9 of *Proceedings of Machine Learning Research*, pp. 297–304, Chia Laguna Resort, Sardinia, Italy, 13–15 May 2010.
- Michael U Gutmann and Aapo Hyvärinen. Noise-contrastive estimation of unnormalized statistical models, with applications to natural image statistics. *Journal of Machine Learning Research*, 13(2), 2012.
- Kyle Hundman, Valentino Constantinou, Christopher Laporte, Ian Colwell, and Tom Soderstrom. Detecting spacecraft anomalies using lstms and nonparametric dynamic thresholding. In *Proceedings of the 24th ACM SIGKDD international conference on knowledge discovery & data mining*, pp. 387–395, 2018.
- Aapo Hyvarinen and Hiroshi Morioka. Unsupervised feature extraction by time-contrastive learning and nonlinear ica. In D. Lee, M. Sugiyama, U. Luxburg, I. Guyon, and R. Garnett (eds.), *Advances in Neural Information Processing Systems*, volume 29. Curran Associates, Inc., 2016a.
- Aapo Hyvarinen and Hiroshi Morioka. Unsupervised feature extraction by time-contrastive learning and nonlinear ica. *arXiv preprint arXiv:1605.06336*, 2016b.
- Brian Kenji Iwana and Seiichi Uchida. An empirical survey of data augmentation for time series classification with neural networks. *Plos one*, 16(7):e0254841, 2021a.
- Brian Kenji Iwana and Seiichi Uchida. Time series data augmentation for neural networks by time warping with a discriminative teacher. In *2020 25th International Conference on Pattern Recognition (ICPR)*, pp. 3558–3565. IEEE, 2021b.
- Krzysztof Kamycki, Tomasz Kapuscinski, and Mariusz Oszust. Data augmentation with suboptimal warping for time-series classification. *Sensors*, 20(1):98, 2020.
- Jin-Hwa Kim, Kyoung-Woon On, Woosang Lim, Jeonghee Kim, Jung-Woo Ha, and Byoung-Tak Zhang. Hadamard product for low-rank bilinear pooling. *arXiv preprint arXiv:1610.04325*, 2016.
- Diederik P. Kingma and Jimmy Ba. Adam: A method for stochastic optimization, 2017.
- K Krishna and M Narasimha Murty. Genetic k-means algorithm. *IEEE Transactions on Systems, Man, and Cybernetics, Part B (Cybernetics)*, 29(3):433–439, 1999.
- Rahul Krishnan, Uri Shalit, and David Sontag. Structured inference networks for nonlinear state space models. In *Proceedings of the AAAI Conference on Artificial Intelligence*, volume 31, 2017.
- Xiang Lan, Dianwen Ng, Shenda Hong, and Mengling Feng. Intra-inter subject self-supervised learning for multivariate cardiac signals, 2021.
- Martin Längkvist, Lars Karlsson, and Amy Loutfi. A review of unsupervised feature learning and deep learning for time-series modeling. *Pattern Recognition Letters*, 42:11–24, 2014.
- Nikolay Laptsev, Saeed Amizadeh, and Ian Flint. Generic and scalable framework for automated time-series anomaly detection. In *Proceedings of the 21th ACM SIGKDD International Conference on Knowledge Discovery and Data Mining*, pp. 1939–1947, New York, NY, USA, 2015.
- Qi Lei, Jinfeng Yi, Roman Vaculin, Lingfei Wu, and Inderjit S Dhillon. Similarity preserving representation learning for time series clustering. *arXiv preprint arXiv:1702.03584*, 2017.
- Yanhao Li, Naiyan Wang, Jiaying Liu, and Xiaodi Hou. Factorized bilinear models for image recognition. In *Proceedings of the IEEE International Conference on Computer Vision*, pp. 2079–2087, 2017.
- Tsung-Yu Lin, Aruni RoyChowdhury, and Subhransu Maji. Bilinear cnn models for fine-grained visual recognition. In *Proceedings of the IEEE international conference on computer vision*, pp. 1449–1457, 2015.

- Xu Liu, Yuxuan Liang, Yu Zheng, Bryan Hooi, and Roger Zimmermann. Spatio-temporal graph contrastive learning. *arXiv preprint arXiv:2108.11873*, 2021.
- Jonathan Long, Evan Shelhamer, and Trevor Darrell. Fully convolutional networks for semantic segmentation. In *Proceedings of the IEEE conference on computer vision and pattern recognition*, pp. 3431–3440, 2015.
- Xinrui Lyu, Matthias Hueser, Stephanie L Hyland, George Zerveas, and Gunnar Raetsch. Improving clinical predictions through unsupervised time series representation learning. *arXiv preprint arXiv:1812.00490*, 2018.
- Qianli Ma, Jiawei Zheng, Sen Li, and Gary W Cottrell. Learning representations for time series clustering. *Advances in neural information processing systems*, 32:3781–3791, 2019.
- Pankaj Malhotra, Vishnu TV, Lovekesh Vig, Puneet Agarwal, and Gautam Shroff. Timenet: Pre-trained deep recurrent neural network for time series classification. *arXiv preprint arXiv:1706.08838*, 2017.
- Aditya P Mathur and Nils Ole Tippenhauer. Swat: A water treatment testbed for research and training on ics security. In *2016 international workshop on cyber-physical systems for smart water networks (CySWater)*, pp. 31–36. IEEE, 2016.
- Tomas Mikolov, Kai Chen, Greg Corrado, and Jeffrey Dean. Efficient estimation of word representations in vector space. *arXiv preprint arXiv:1301.3781*, 2013.
- George Moody. A new method for detecting atrial fibrillation using rr intervals. *Computers in Cardiology*, pp. 227–230, 1983.
- Aaron van den Oord, Yazhe Li, and Oriol Vinyals. Representation learning with contrastive predictive coding. *arXiv preprint arXiv:1807.03748*, 2018.
- Boris N. Oreshkin, Dmitri Carpov, Nicolas Chapados, and Yoshua Bengio. N-beats: Neural basis expansion analysis for interpretable time series forecasting. In *International Conference on Learning Representations*, 2020.
- Matteo Pagliardini, Prakhar Gupta, and Martin Jaggi. Unsupervised learning of sentence embeddings using compositional n-gram features. In *Proceedings of the 2018 Conference of the North American Chapter of the Association for Computational Linguistics: Human Language Technologies, Volume 1 (Long Papers)*, pp. 528–540, 2018.
- Adam Paszke, Sam Gross, Soumith Chintala, Gregory Chanan, Edward Yang, Zachary DeVito, Zeming Lin, Alban Desmaison, Luca Antiga, and Adam Lerer. Automatic differentiation in pytorch. 2017.
- Nitish Srivastava, Geoffrey Hinton, Alex Krizhevsky, Ilya Sutskever, and Ruslan Salakhutdinov. Dropout: A simple way to prevent neural networks from overfitting. *Journal of Machine Learning Research*, 15(56):1929–1958, 2014.
- Ya Su, Youjian Zhao, Chenhao Niu, Rong Liu, Wei Sun, and Dan Pei. Robust anomaly detection for multivariate time series through stochastic recurrent neural network. In *Proceedings of the 25th ACM SIGKDD International Conference on Knowledge Discovery & Data Mining*, pp. 2828–2837, 2019.
- Sana Tonekaboni, Danny Eytan, and Anna Goldenberg. Unsupervised representation learning for time series with temporal neighborhood coding. *arXiv preprint arXiv:2106.00750*, 2021.
- Laurens Van der Maaten and Geoffrey Hinton. Visualizing data using t-sne. *Journal of machine learning research*, 9(11), 2008.
- Ashish Vaswani, Noam Shazeer, Niki Parmar, Jakob Uszkoreit, Llion Jones, Aidan N Gomez, Łukasz Kaiser, and Illia Polosukhin. Attention is all you need. In *Advances in neural information processing systems*, pp. 5998–6008, 2017.

- Tongzhou Wang and Phillip Isola. Understanding contrastive representation learning through alignment and uniformity on the hypersphere. In *International Conference on Machine Learning*, pp. 9929–9939. PMLR, 2020.
- Xiaolong Wang and Abhinav Gupta. Unsupervised learning of visual representations using videos. In *Proceedings of the IEEE international conference on computer vision*, pp. 2794–2802, 2015.
- Xing Wei, Yue Zhang, Yihong Gong, Jiawei Zhang, and Nanning Zheng. Grassmann pooling as compact homogeneous bilinear pooling for fine-grained visual classification. In *Proceedings of the European Conference on Computer Vision (ECCV)*, pp. 355–370, 2018.
- Chaojian Yu, Xinyi Zhao, Qi Zheng, Peng Zhang, and Xinge You. Hierarchical bilinear pooling for fine-grained visual recognition. In *Proceedings of the European conference on computer vision (ECCV)*, pp. 574–589, 2018.
- Zhihan Yue, Yujing Wang, Juanyong Duan, Tianmeng Yang, Congrui Huang, and Bixiong Xu. Learning timestamp-level representations for time series with hierarchical contrastive loss. *arXiv preprint arXiv:2106.10466*, 2021.
- George Zerveas, Srideepika Jayaraman, Dhaval Patel, Anuradha Bhamidipaty, and Carsten Eickhoff. A transformer-based framework for multivariate time series representation learning. In *Proceedings of the 27th ACM SIGKDD Conference on Knowledge Discovery & Data Mining*, pp. 2114–2124, 2021.
- Haoyi Zhou, Shanghang Zhang, Jieqi Peng, Shuai Zhang, Jianxin Li, Hui Xiong, and Wancai Zhang. Informer: Beyond efficient transformer for long sequence time-series forecasting, 2021.



## A APPENDIX

### A.1 VISUALIZATION

To make assessments about the clusterability of learned representations in the encoding space, we visualize the feature distribution by using t-SNE (Van der Maaten & Hinton, 2008). It is noted that if the information of the latent state is properly learned and encoded by the model, the representations from the same underlying state should cluster together. Figure 6 shows the comparisons about representations distribution of different models. It demonstrates that the representations learned by proposed BTSF from the same hidden state are better than the other approaches. The visualization results further prove the superior representation ability of our model. In Addition, we have evaluated on the all univariate time series datasets: the UCR archive. The corresponding critical difference diagram is shown in Figure 7. The BTSF significantly outperforms the other approaches with an average rank of almost 1.3.

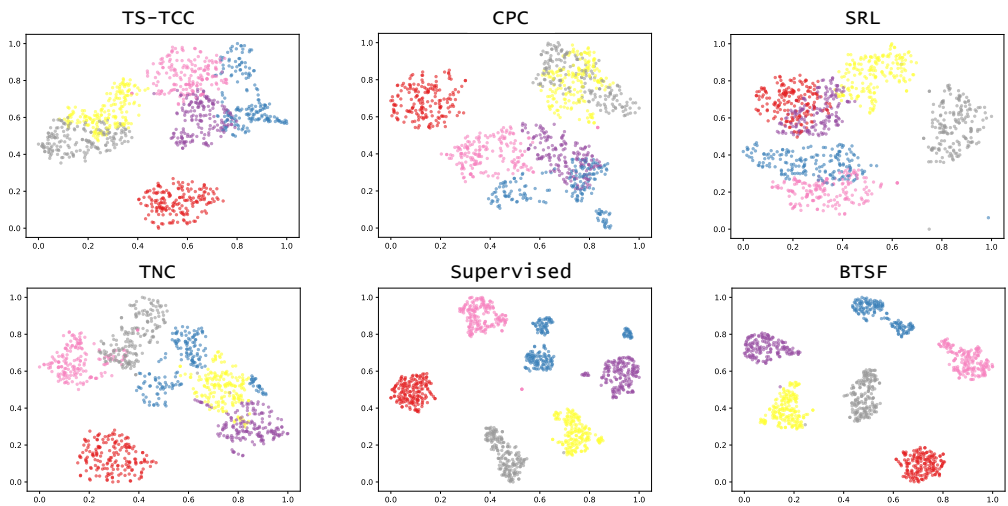


Figure 6: T-SNE visualization of signal representations for HAR dataset.

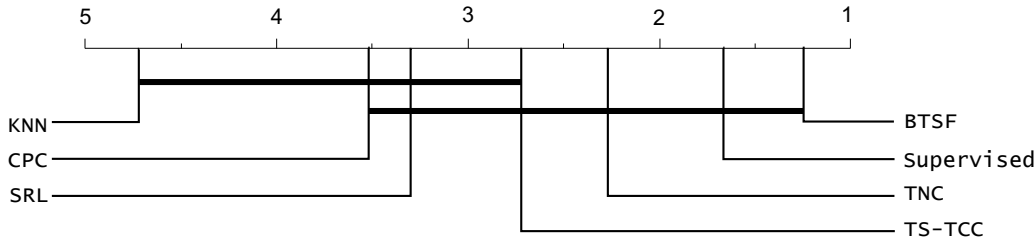


Figure 7: Critical difference diagram showing pairwise statistical difference comparison of BTSF and previous methods on the UCR archive.

### A.2 EFFECTIVENESS

To prove the efficiency of our devised bilinear fusion, we provide the deduction of gradient flow from the loss function. Since the overall architecture is a directed acyclic graph, the parameters can be trained by back-propagating the gradients of the contrastive loss. The bilinear form simplifies the gradient computations. Let  $\frac{\partial \mathcal{L}}{\partial \mathbf{f}}$  be the gradient of  $\mathcal{L}$  with respect to  $\mathbf{f}$ , then for Eq.(8) by chain rule

Table 6: Ablation experiments of BTSF.

Accuracy	Temporal	Spectral	Sum/Concat	Bilinear	Iterative Bilinear
Slicing	88.3	86.7	88.7	90.7	91.5
Dropout	89.4	88.4	89.8	92.4	<b>94.6</b>
Layer-Wise Dropout	89.8	89.1	90.4	93.1	<b>95.4</b>

of gradients we can get:

$$\frac{\partial \mathcal{L}}{\partial \mathbf{F}_t} = \frac{\partial \mathcal{L}}{\partial \mathbf{f}} \mathbf{W}_t + 2 \frac{\partial \mathcal{L}}{\partial \mathbf{f}} \mathbf{W} \mathbf{F}_s, \quad \frac{\partial \mathcal{L}}{\partial \mathbf{F}_s} = \frac{\partial \mathcal{L}}{\partial \mathbf{f}} \mathbf{W}_s + 2 \frac{\partial \mathcal{L}}{\partial \mathbf{f}} \mathbf{W} \mathbf{F}_t \quad (10)$$

$$\frac{\partial \mathcal{L}}{\partial \mathbf{W}_t} = \frac{\partial \mathcal{L}}{\partial \mathbf{f}} \mathbf{F}_t, \quad \frac{\partial \mathcal{L}}{\partial \mathbf{W}_s} = \frac{\partial \mathcal{L}}{\partial \mathbf{f}} \mathbf{F}_s, \quad \frac{\partial \mathcal{L}}{\partial \mathbf{W}} = \frac{\partial \mathcal{L}}{\partial \mathbf{f}} \mathbf{F}_t \mathbf{F}_s^T \quad (11)$$

$$\frac{\partial \mathcal{L}}{\partial \theta_t} = \frac{\partial \mathcal{L}}{\partial \mathbf{f}} \frac{\partial \mathbf{f}}{\partial \theta_t} \mathbf{W}_t + 2 \frac{\partial \mathcal{L}}{\partial \mathbf{f}} \frac{\partial \mathbf{f}}{\partial \theta_t} \mathbf{W} \mathbf{F}_s, \quad \frac{\partial \mathcal{L}}{\partial \theta_s} = \frac{\partial \mathcal{L}}{\partial \mathbf{f}} \frac{\partial \mathbf{f}}{\partial \theta_s} \mathbf{W}_s + 2 \frac{\partial \mathcal{L}}{\partial \mathbf{f}} \frac{\partial \mathbf{f}}{\partial \theta_s} \mathbf{W} \mathbf{F}_t \quad (12)$$

From the Eq.(10) and Eq.(12), we conclude that the gradient update of parameters  $\theta_t$  in temporal feature  $\mathbf{F}_t$  is closely related to the spectral feature since  $\mathbf{F}_s$  is treated as a weighted coefficient straightly multiplying the gradient, and vice versa. Additionally, we can know that interaction matrix  $\mathbf{W}$  has a strong connection with cross-domain affinities  $\mathbf{F}_t \mathbf{F}_s^T$  from the Eq.(11) which leads to a better combination of temporal and spectral features. In hence, it is proved that our BTSF adequately explores and utilizes the underlying spectral and temporal information of time series.

### A.3 MORE ABLATION STUDIES

To quantify the promotion of each module in BTSF, we make a specific ablation study where all experiments are conducted on HAR dataset and results are in Table 6. We use TNC as a baseline which applies time slicing as augmentation with accuracy of 88.3%. We could find that our instance-level augmentation (dropout) is better than segment-level augmentation (slicing) and layer-wise dropout (adding dropout in internal layers) has a promotion by 1.5% compared with slicing. However, we do not apply layer-wise dropout in aforementioned experiments for fair comparisons otherwise our BTSF will have better performance. Besides, incorporating spectral feature with temporal feature by using summation or concatenation will also improve the results, which illustrates the necessity of cross-domain interaction. The accuracy is obviously promoted by 2%~3% when involving temporal and spectral information with bilinear fusion, and iterative operation will further improve the performance by enhancing and refining the temporal-spectral interaction. In conclusion, instance-level augmentation (dropout) and iterative bilinear fusion are two main modules of BTSF which largely improve the generalization ability of unsupervised learned representations with accuracy of 94.6%, an improvement of 6.3% to baseline.

**Studies of hyperparameters** In the proposed BTSF, there are some hyperparameters needed to be carefully set, the dropout rate, temperature number  $\tau$  and the loops number of iterative bilinear fusion. Table 7 illustrates that when the rate is set to 0.1, BTSF acquires the best performance since setting too high value would lose the original properties of time series and setting too low value would bring about representation collapse. Table 8 demonstrates that when  $\tau$  is set to 0.05, BTSF has the best performance. It is reasonable that proper value of  $\tau$  would promote the optimization of training process and make representations more discriminative with the adjustment. We also run the experiments of loops number of iterative bilinear fusion and the results are depicted in Figure 8. From the results, we conclude that our iterative bilinear fusion is effective and its performance converges after just three loops.

### A.4 DATASETS DESCRIPTIONS AND MORE EXPERIMENTS

In all experiments, we use Pytorch 1.8.1 (Paszke et al., 2017) and train all the models on a GeForce RTX 2080 Ti GPU with CUDA 10.2. We apply an Adam optimizer (Kingma & Ba, 2017) with

Table 7: Ablation experiments of dropout rate

dropout rate	p=0.01	p=0.05	p=0.1	p=0.15	p=0.2	p=0.3
HAR	90.29	92.78	<b>94.63</b>	93.36	91.21	88.07
Sleep-EDF	82.76	85.34	<b>87.45</b>	86.01	83.44	80.92
ECG Waveform	93.13	96.56	<b>98.12</b>	97.28	95.63	92.05

Table 8: Ablation experiments on temperature number  $\tau$ .

$\tau$	0.001	0.01	0.05	0.1	1
HAR	90.04	92.91	<b>94.63</b>	93.04	91.85
Sleep-EDF	82.69	84.82	<b>87.45</b>	85.11	83.28
ECG Waveform	93.06	95.74	<b>98.12</b>	96.47	94.88

a learning rate of  $3e-4$ , weight decay of  $1e-4$  and batch size is set to 256. In this part, we would introduce all the datasets used in our experiments which involve three kinds of downstream tasks, time series classification, forecasting and anomaly detection. The definitions of downstream tasks are detailed in the following:

- **Time Series Classification:** Given the univariate time series  $\{x_1, x_2, \dots, x_T\}$  or multivariate time series  $\{\mathbf{x}_1, \mathbf{x}_2, \dots, \mathbf{x}_D\}$  as input, time series classification is to classify the input consisting of real-valued observations to a certain class.
- **Time Series Forecasting:** Given the past univariate observations  $\{x_{t-T_1+1}, \dots, x_t\}$  or multivariate ones  $\{\mathbf{x}_{t-T_1+1}, \dots, \mathbf{x}_t\}$  as input, time series forecasting aims to predict the future data points  $\{x_{t+1}, x_{t+2}, \dots, x_{t+T_2}\}$  or  $\{\mathbf{x}_{t+1}, \mathbf{x}_{t+2}, \dots, \mathbf{x}_{t+T_2}\}$  based on the input.
- **Time Series Anomaly Detection:** Given the univariate time series  $\{x_1, x_2, \dots, x_T\}$  or multivariate time series  $\{\mathbf{x}_1, \mathbf{x}_2, \dots, \mathbf{x}_D\}$  as input, time series anomaly detection is to find out which point ( $\hat{x}_i$  or  $\hat{\mathbf{x}}_i$ ) or subsequence ( $\{\hat{x}_1, \hat{x}_2, \dots, \hat{x}_T\}$  or  $\{\hat{\mathbf{x}}_1, \hat{\mathbf{x}}_2, \dots, \hat{\mathbf{x}}_T\}$ ) of the input behaves unusually when compared either to the other values in the time series (global outlier) or to its neighboring points (local outlier).

**Data Preprocessing** Following Franceschi et al. (2019); Zhou et al. (2021), for univariate time series classification task, we normalize datasets using z-score so that the set of observations for each dataset has zero mean and unit variance. For multivariate time series classification task, each variable is normalized independently using z-score. For forecasting tasks, all reported metrics are calculated based on the normalized time series.

#### A.4.1 CLASSIFICATION

In the time series classification task, we choose six popular datasets which are widely used in previous works. These six datasets are Human Activity Recognition (HAR) (Anguita et al., 2013), Sleep Stage Classification (Sleep-EDF) (Goldberger et al., 2000), Epilepsy Seizure Prediction (Andrzejak et al., 2001), ECG Waveform (Moody, 1983), UCR (Dau et al., 2019) and UEA (Bagnall et al., 2018). The detailed introduction to these datasets are as follows:

**Human Activity Recognition** HAR dataset contains 30 individual subjects which provide six activities for each subject. These six activities are walking, walking upstairs, downstairs, standing, sitting, and lying down. The data of HAR is collected by sensors with a sampling rate of 50 HZ and the collected signals record the continuous activity of every subject.

**Sleep Stage Classification** The dataset is designed for EEG signal classification task where each signal belongs to one of five categories: Wake (W), Non-rapid eye movement (N1, N2, N3) and Rapid Eye Movement (REM). And the Sleep-EDF dataset collects the PSG for the whole night, and we just used a single EEG channel, following previous works (Eldele et al., 2021a).

**Epilepsy Seizure Prediction** The Epileptic Seizure Prediction dataset contains EEG signals which are collected from 500 subjects. The brain activity for each subject was recorded for 23.6 seconds.

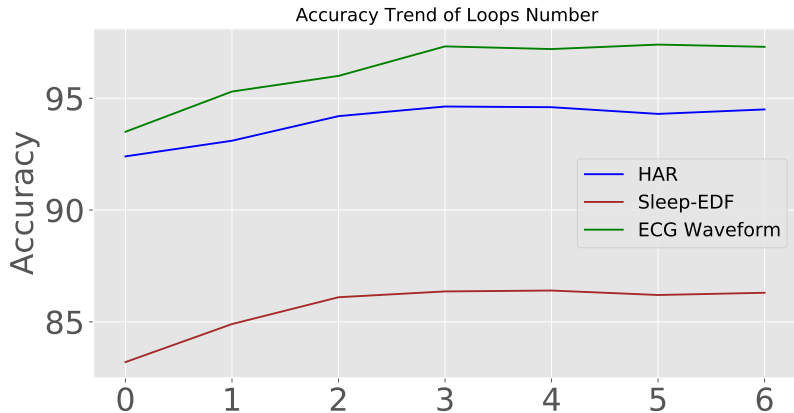


Figure 8: Accuracy trend of changing loops number on HAR, Sleep-EDF and ECG Waveform datasets.

Table 9: More comparisons of classification results about BTSF and previous work, results of TST (Zerveas et al., 2021), Rocket (Dempster et al., 2020) and Supervised (Zerveas et al., 2021) are quoted from TST for fair comparisons.

Methods	TST	Rocket	Supervised	<b>BTSF</b>
EthanolConcentration	32.6	45.2	33.7	<b>49.4</b>
FaceDetection	68.9	64.7	68.1	<b>73.0</b>
Handwriting	35.9	58.8	30.5	<b>62.3</b>
Heartbeat	77.6	75.6	77.6	<b>84.7</b>
JapaneseVowels	99.7	96.2	99.4	<b>99.8</b>
InsectWingBeat	68.7	-	68.4	<b>78.3</b>
PEMS-SF	89.6	75.1	91.9	<b>95.7</b>
SelfRegulationSCP1	92.2	90.8	92.5	<b>96.5</b>
SelfRegulationSCP2	60.4	53.3	58.9	<b>64.9</b>
SpokenArabicDigits	99.8	71.2	99.3	<b>99.8</b>
UWaveGestureLibrary	91.3	94.4	90.3	<b>97.1</b>
<b>Avg Accuracy</b>	74.8	72.5	74.2	<b>82.0</b>
<b>Avg Rank</b>	1.7	2.3	1.7	<b>1.2</b>

Additionally, the original classes of the dataset are five, and we preprocess the dataset for classification task like Eldede et al. (2021b).

**ECG Waveform** The ECG Waveform is a real-world clinical dataset, it includes 25 long-term Electrocardiogram (ECG) recordings (10 hours in duration) of human subjects with atrial fibrillation. Besides, it contains two ECG signals with a sampling rate of 250HZ.

**UCR and UEA** The UCR and UEA are widely used public datasets for time series analysis. The UCR archive consists of univariate datasets while UEA archive contains multivariate datasets, which cover multiple scenes in real world.

Table 9 shows the comparison results between BTSF with recent works following their evaluation protocols. The results show that BTSF significantly outperforms them in a large margin. Table 10 shows the classification results of Epileptic Seizure Prediction datasets. From the illustrated results, we conclude that our BTSF gets the best performance and exceeds other methods by a large margin in univariate and multivariate time series classification tasks.

Table 10: More comparisons of classification results of ESP dataset.

Methods	Epilepsy Seizure Prediction	
	Accuracy	AUPRC
Supervised	96.32±0.38	0.97±0.65
KNN	87.96±1.32	0.89±1.04
SRL	94.65±0.97	0.95±0.86
CPC	96.61±0.43	0.97±0.69
TS-TCC	97.23±0.10	0.98±0.21
TNC	96.15±0.33	0.96±0.45
<b>BTSF</b>	<b>99.01±0.12</b>	<b>0.99±0.06</b>

#### A.4.2 FORECASTING

In Section 4, we conduct experiments on four datasets about time series forecasting, including two collected real-world datasets for long sequence time-series forecasting (LSTF) problem and one public benchmark dataset as in Zhou et al. (2021). The detailed introduction to these datasets are as follows:

**Electricity Transformer Temperature (ETT)** The ETT is a crucial indicator in the electric power long-term deployment. The 2-year data was collected from two separated counties in China, which was first used to investigate the granularity on the LSTF problem with each data point containing the target value "oil temperature" and six power load features. ETTh1, ETTh2 and ETTm1 represent for 1-hour-level and 15-minute-level respectively.

**Weather** This dataset contains local climatological data for about 1,600 U.S. places, 4 years from 2010 to 2013, where data points are collected every 1 hour with each data point consisting of the target value "wet bulb" and 11 climate features.

We run the forecasting tasks about prediction length of 48 and 1440 on ETT dataset and visualize the forecasting results of BTSF, TNC and supervised models. From Figure 9 and 10, we could find that our BTSF achieves the best forecasting results under both short-term and long-term settings since it adequately leverages the global context and utilize temporal-spectral relations which are helpful in producing more accurate predictive representations. The complete comparisons of forecasting results in Table 11 further prove the superiority of BTSF.

#### A.4.3 ANOMALY DETECTION

In Section 4, we conduct extensive experiments about time series anomaly detection on five widely used datasets, which are all public available. The detailed introduction to these datasets are illustrated as follows:

**Secure Water Treatment (SWaT)** The SWaT dataset is a scaled down version of a real-world industrial water treatment plant producing filtered water (Goh et al., 2016). The collected dataset (Mathur & Tippenhauer, 2016) consists of 11 days of continuous operation: 7 days collected under normal operations and 4 days collected with attack scenarios.

**Water Distribution (WADI)** This dataset is collected from an extension of the SWaT tesbed. It consists of 16 days of continuous operation: 14 days were collected under normal operation and 2 days with attack scenarios.

**Server Machine Dataset (SMD)** This dataset is a 5-week-long dataset from a large internet company which was collected and made publicly available (Su et al., 2019). It contains data from 28 server machines with each one monitored by  $m=33$  metrics. SMD is divided into two subsets of equal size: the first half is the training set and the second half is the testing set.

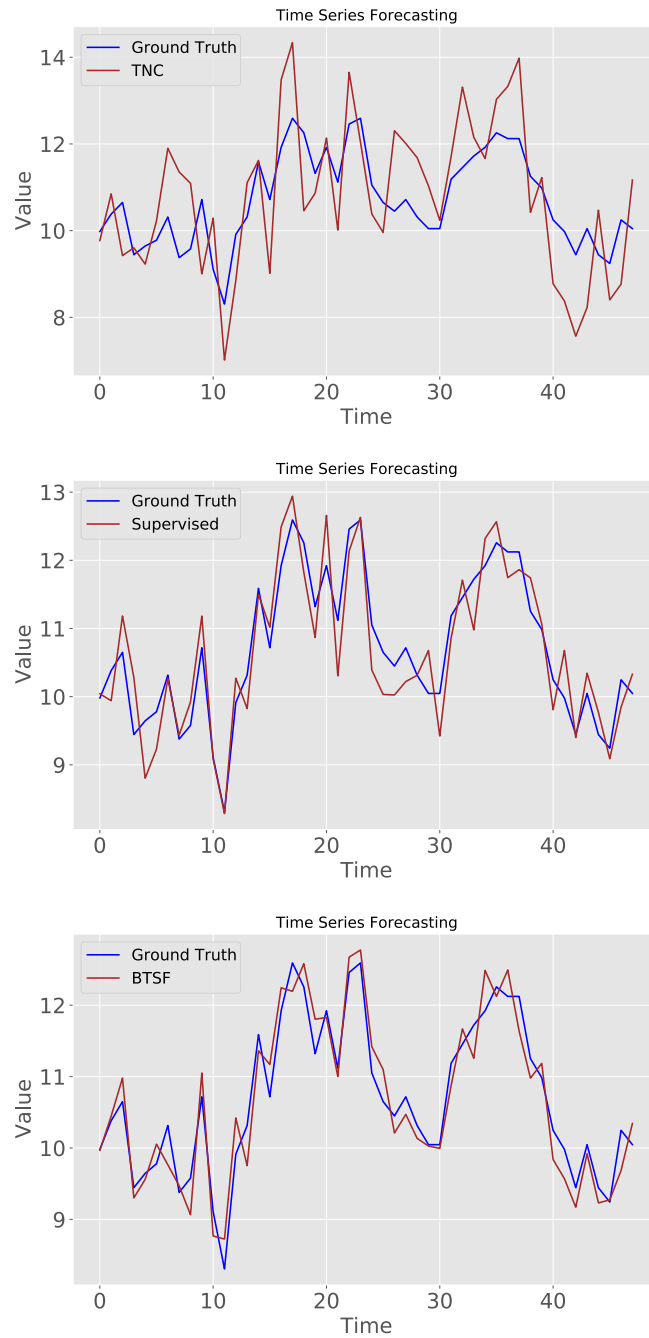


Figure 9: Visualizing forecasting results of length 48 on ETT dataset.

**Soil Moisture Active Passive (SMAP) and Mars Science Laboratory (MSL)** SMAP and MSL are two real-world public datasets, expert-labeled datasets from NASA (Hundman et al., 2018). They contain respectively the data of 55/27 entities each monitored by  $m = 25/55$  metrics.

The complete comparisons of all metrics (P, R and F1) in anomaly detection are illustrated in Table 12. Our BTSF outperforms other methods including supervised method in a large margin. It demonstrates BTSF is more sensitive to the outliers in time series.



Table 11: Comparisons of multivariate forecasting Results.

Datasets	Length	Supervised		SRL		CPC		TS-TCC		TNC		BTSF	
		MSE	MAE	MSE	MAE	MSE	MAE	MSE	MAE	MSE	MAE	MSE	MAE
ETTh1	24	0.577	0.549	0.698	0.661	0.687	0.634	0.653	0.610	0.632	0.596	<b>0.541</b>	<b>0.519</b>
	48	0.685	0.625	0.758	0.711	0.779	0.768	0.720	0.693	0.705	0.688	<b>0.613</b>	<b>0.524</b>
	168	0.931	0.752	1.341	1.178	1.282	1.083	1.129	1.044	1.097	0.993	<b>0.640</b>	<b>0.532</b>
	336	1.128	0.873	1.578	1.276	1.641	1.201	1.492	1.076	1.454	0.919	<b>0.864</b>	<b>0.689</b>
	720	1.215	0.896	1.892	1.566	1.803	1.761	1.603	1.206	1.604	1.118	<b>0.993</b>	<b>0.712</b>
ETTh2	24	0.720	0.665	1.034	0.901	0.981	0.869	0.883	0.747	0.830	0.756	<b>0.359</b>	<b>0.432</b>
	48	1.451	1.001	1.854	1.542	1.732	1.440	1.701	1.378	1.689	1.311	<b>0.544</b>	<b>0.527</b>
	168	3.389	1.515	5.062	2.167	4.591	3.126	3.956	2.301	3.792	2.029	<b>1.669</b>	<b>0.875</b>
	336	2.723	1.340	4.921	3.012	4.772	3.581	3.992	2.852	3.516	2.812	<b>1.954</b>	<b>1.093</b>
	720	3.467	1.473	5.301	3.207	5.191	2.781	4.732	2.345	4.501	2.410	<b>2.566</b>	<b>1.276</b>
ETTm1	24	0.323	0.369	0.561	0.603	0.540	0.513	0.473	0.490	0.429	0.455	<b>0.302</b>	<b>0.342</b>
	48	0.494	0.503	0.701	0.697	0.727	0.706	0.671	0.665	0.623	0.602	<b>0.395</b>	<b>0.387</b>
	96	0.678	0.614	0.901	0.836	0.851	0.793	0.803	0.724	0.749	0.731	<b>0.438</b>	<b>0.399</b>
	288	1.056	0.786	2.471	1.927	2.066	1.634	1.958	1.429	1.791	1.356	<b>0.675</b>	<b>0.429</b>
	672	1.192	0.926	2.042	1.803	1.962	1.797	1.838	1.601	1.822	1.692	<b>0.721</b>	<b>0.643</b>
Weather	24	0.335	0.381	0.688	0.701	0.647	0.652	0.572	0.603	0.484	0.513	<b>0.324</b>	<b>0.369</b>
	48	0.395	0.459	0.751	0.883	0.720	0.761	0.647	0.691	0.608	0.626	<b>0.366</b>	<b>0.427</b>
	168	0.608	0.567	1.204	1.032	1.351	1.067	1.117	0.962	1.081	0.970	<b>0.543</b>	<b>0.477</b>
	336	0.702	0.620	2.164	1.982	2.019	1.832	1.783	1.370	1.654	1.290	<b>0.568</b>	<b>0.487</b>
	720	0.831	0.731	2.281	1.994	2.109	1.861	1.850	1.566	1.401	1.193	<b>0.601</b>	<b>0.522</b>

Table 12: Comparisons of multivariate anomaly detection.

Datasets	Metric	Supervised	SRL	CPC	TS-TCC	TNC	BTSF
SAaT	P	0.996	0.784	0.791	0.823	0.816	<b>0.997</b>
	R	0.842	0.603	0.644	0.712	0.726	<b>0.873</b>
	F1	0.901	0.710	0.738	0.775	0.799	<b>0.944</b>
WADI	P	0.720	0.459	0.473	0.522	0.561	<b>0.763</b>
	R	0.761	0.478	0.492	0.525	0.574	<b>0.801</b>
	F1	0.649	0.340	0.382	0.427	0.440	<b>0.685</b>
SMD	P	0.984	0.751	0.783	0.802	0.834	<b>0.993</b>
	R	0.963	0.790	0.774	0.811	0.806	<b>0.985</b>
	F1	0.958	0.768	0.732	0.794	0.817	<b>0.972</b>
SMAP	P	0.791	0.562	0.597	0.639	0.641	<b>0.881</b>
	R	0.985	0.755	0.781	0.812	0.826	<b>0.994</b>
	F1	0.842	0.598	0.620	0.679	0.693	<b>0.906</b>
MSL	P	0.937	0.728	0.778	0.825	0.819	<b>0.968</b>
	R	0.980	0.702	0.749	0.793	0.815	<b>0.993</b>
	F1	0.945	0.788	0.813	0.795	0.833	<b>0.984</b>

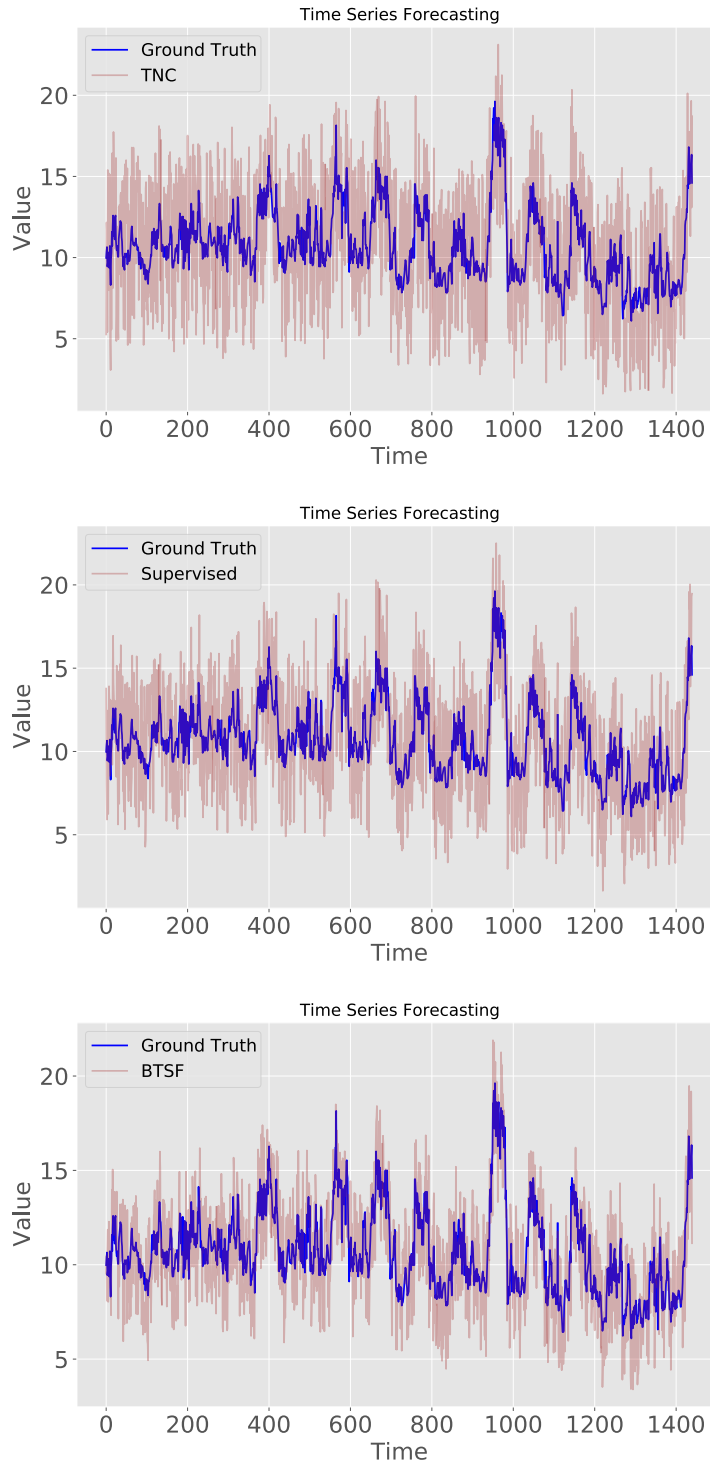


Figure 10: Visualizing long-term forecasting results of length 1440 on ETT dataset.